Raman spectra on TDAE-C_{60} single crystals

K. Pokhodnia,* J. Demsar, A. Omerzu, and D. Mihailovic
''Jozef Stefan'' Institute, Jamova 39, Ljubljana, Slovenia

H. Kuzmany
Universität Wien, Institut für Festkörperphysik, Strudlhofgasse 4, A-1090 Wien, Austria

(Received 9 July 1996)

Low-temperature single-crystal Raman spectra are presented for the organic ferromagnetic insulator TDAE-C_{60}. The mode intensities, line shifts, linewidths, and depolarization ratios are compared with alkali-doped fullerene materials and with pure C_{60}. A comparison of visible laser light excited spectra ($E_{exc}=2.41$ eV) with infrared excited Raman measurements ($E_{exc}=1.17$ eV) shows a selective resonance effect whereby in the visible spectra, a frequency shift of *only the tangential modes* is observed, while in the infrared measurement, which is resonant with the t_{1u}-t_{1g} electronic transition, the *radial modes* are also observed to shift. The effect is attributed to Raman resonance with different relaxed states of C_{60}^{-}. [S0163-1829(97)01206-X]

I. INTRODUCTION

The relatively small changes of the vibrational and electronic properties of a C_{60} molecule in many fullerene-based compounds were often considered as an indication of the weak interaction between adjacent buckyballs in the solid state. However, there is appreciable interest in systems where this interaction should play an important role in determining the macroscopic properties. The molecular charge transfer complex TDAE-C_{60} [where TDAE is tetrakis (dimethylamino)ethylene, $C_2N_4(CH_3)_8$] is one of such examples. It has become a subject of intensive study after the discovery of a possibly ferromagnetic transition at $T_c=16$ K.[1] This transition temperature is the highest for all known nonpolymeric purely organic ferromagnets.

TDAE-C_{60} crystallizes in a monoclinic unit cell belonging to $C2/c$ space group with four chemically equivalent formula units.[2] The shortest C_{60}-C_{60} distance is 9.95 Å (along the c direction) which implies that there are no polymer bondings between the neighboring C_{60} ions as it was suggested for the orthorhombic phase of alkali-metal-doped C_{60} compounds MC_{60} (M=K,Rb).[3] Magnetic resonance measurements on TDAE-C_{60} have shown that the unpaired electron is mainly localized at the C_{60} ion.[4] In spite of the fact that the HOMO level of TDAE-C_{60} is partially filled and a metallic ground state might be expected, the transport measurements down to 110 K showed insulating behavior with phonon-assisted polaronic hopping between relatively weak coupled C_{60} ions.[5]

On the other hand, ESR and NMR studies have indicated the importance of the electron correlations even above T_c. Strong line narrowing was observed in the ESR spectra of TDAE-C_{60} single crystals below the C_{60} rotation freezing temperature ($\sim$150 K) (Ref. 6) attributed most probably to exchange narrowing. Presuming that C_{60}^{-} ions can undergo a Jahn-Teller distortion below this temperature, it was suggested that the origin of the weak ferromagnetism in TDAE-C_{60} is a superposition of the direct antiferromagnetic coupling between C_{60}^{-} along the c direction and TDAE-assisted indirect coupling in the perpendicular direction giving rise to a spin canting.[6,7] It was also shown that the ferromagnetic properties of TDAE-C_{60} depend on the degree of the orientational ordering of the C_{60} ions.[8]

Due to the high I_h symmetry of the C_{60} molecule, group theory predicts only 10 Raman-active modes and four infrared-active ones, despite 174 degrees of freedom for carbon atoms. Thus, any symmetry reduction of C_{60} ions in TDAE-C_{60} should reveal itself in the appearance of silent modes not active for isolated icosahedra, including odd parity vibrations as it was observed in the MC_{60} Raman spectra below 397 K (Ref. 9) and in the new phases of C_{60} synthesized at a high pressure.[10]

The early Raman and infrared absorption measurements of TDAE-C_{60} were performed on powder samples or doped C_{60} films.[11–13] A signal-to-noise ratio in these measurements was not very good, especially at low temperatures. The

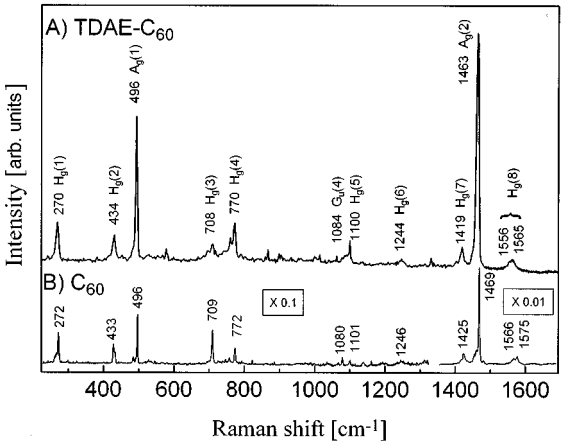

FIG. 1. The Raman spectra of the TDAE-C_{60} single crystal compared to undoped C_{60} single crystal at 10 K using 514.5 nm laser excitation. Red shift and broadening of $A_g(2)$ pinch mode and H_g modes can be observed.

TABLE I. Observed Raman modes of TDAE-C_{60} crystal at 10 K compared to observed modes of pure C_{60} and to Raman modes of TDAE-C_{60} powder measured by Denisov *et al.* (Ref. 12) at $T=300$ K and $\lambda=1064$ nm. The modes are assigned according to the modes of free C_{60} molecule and the number in parantheses is the percentage of radial mode character calculated by Stanton and Newton (Ref. 17). Frequency ω, linewidth (FWHM), relative intensities, and depolarization ratio $\rho=I_{\parallel\perp}/I_{\parallel\parallel}$ of these modes are shown.

I_h modes	C_{60} Single crystal			TDAE-C_{60} Single crystal				TDAE-C_{60} Powder
	ω (cm^{-1})	FWHM (cm^{-1})	Rel. int.	ω (cm^{-1})	FWHM (cm^{-1})	Rel. int.	ρ	ω (cm^{-1})
$A_g(1)$ (100)	496	2.5	100	496	8	100	0.1	491
	1455	4	30	-	-	-	-	-
	1461	4	28	1457	7.5	30	0.15	-
$A_g(2)$ (0)	1469	3	360	1463	7.7	230	0.12	-
	262	3	10	255	32	55	-	-
	266	5	30	265	4	15	-	-
$H_g(1)$ (69.3)	272	3	70	270	8.5	65	0.25	263
	428	3.5	45	427	4	40	0.4	424
$H_g(2)$ (90.0)	433	5	15	434	8.5	75	0.3	-
$H_g(3)$ (96.5)	709	3.5	125	708	18	16	0.3	697
$H_g(4)$ (30.5)	773	4	55	769	7	24	0.2	771
$H_g(5)$ (9.6)	1101	5	23	1100	7	4	-	1099
$H_g(6)$ (2.1)	1246	4	7	1244	13	12	0.6	1245
	1417	6	8	-	-	-	-	1414
	1424	5	45	1420	10	19	0.5	-
$H_g(7)$ (0.8)	1433	11	180	-	-	-	-	-
	1566	16	210	1556	19	22	-	1558
$H_g(8)$ (1.2)	1575	7	120	1565	8	32	-	-
$G_g(1)$	484	4	33	487	10	25	0.4	-
$Hg(1)\oplus Gg(1)$	758	6	20	759	8	12	-	
$G_u(4)$	1080	4	8	1084	16.5	14	-	

charge-frequency correlation curve for the $A_g(2)$ mode of C_{60}^{-n} ($n=0,1,3,4,6$) suggests a softening of eight wave numbers,[14,15] but the shift of this mode was found to be either higher[11] or lower[13] than the expected value. Also a strong dependence of the $A_g(2)$ mode position and intensity upon the laser power was observed.[13] On the other hand, it is known that some amount of unreacted C_{60} could remain in the powder sample or in the incompletely doped C_{60} film.[13] Taking into account that the resonance cross section of the $A_g(2)$ mode excited with a green laser line in C_{60} is apparently much higher than in TDAE-C_{60}, even a small amount of unreacted C_{60} or photodegradation effects can considerably distort the real spectrum. Thus, the experiments performed on the crystalline TDAE-C_{60} are of great importance.

In the present work the Raman spectra of TDAE-C_{60} single crystals were studied at temperatures well below the temperature of the orientation ordering transition. A red shift of the $A_g(2)$ pentagonal pinch mode of 6 ± 1 cm^{-1} was observed, which is in a good agreement with MC_{60} results.[14,15] The broadening and splitting of the degenerate modes is clearly seen at low temperatures. In contrast to polymer or pressure induced phases of C_{60}, we see no C_{60} symmetry breaking, but effects due to resonance with the $h_u\rightarrow t_{1g}$, HOMO-1$\rightarrow$LUMO electronic transition are observed and compared with Raman experiments resonant with the $t_{1u}\rightarrow t_{1g}$, HOMO-LUMO transition.

II. EXPERIMENT

The TDAE-C_{60} single crystals were grown in our laboratory from solution of C_{60} and TDAE in toluene by the diffusion method. Fullerene C_{60} (Hoechst, 99.4%) and TDAE (Aldrich, 97%) were taken for crystal growth as purchased. All manipulations were performed in an argon glove box (oxygen concentration less than 1 ppm). Shiny black crystals with well-developed faces of typical sizes $0.5\times1\times1.5$ mm were obtained after 2–3 weeks. The existence of a ferromagnetic transition at 16 K in the crystals was confirmed by ESR measurements.

Since TDAE-C_{60} is highly reactive with oxygen, special care was taken to protect the surface of the crystals from exposition to air. The single crystals of TDAE-C_{60} were glued on the cold finger of the CF2102 Oxford cryostat (using Torr Seal epoxy glue) in the argon glove box. The cryostat was afterwards evacuated to the high vacuum ($\sim10^{-6}$ mbar). To avoid a systematic error in the evaluation of the C_{60} ionization shift of the Raman modes in TDAE-C_{60}, the position of the same mode was always measured simultaneously for a C_{60} single crystal which was attached near the investigated TDAE-C_{60} sample.

In order to obtain the Raman spectra of TDAE-C_{60} crystals, resonant excitation with the $h_u\rightarrow t_{1g}$ transition of C_{60} an argon-ion laser (Coherent Innova 70) line at $\lambda=514.5$ nm

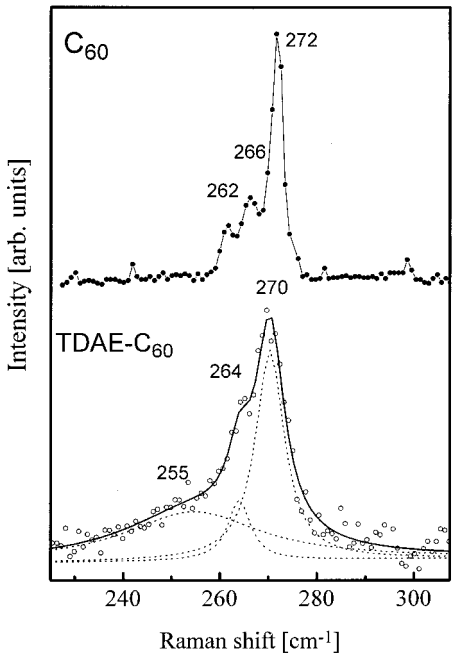

FIG. 2. The asymmetric line of the $H_g(1)$ mode at 270 cm^{-1} is fit by the sum of three Lorentzians centered at 255, 264, and 270 cm^{-1}, respectively. The data are shown by dots, while the solid line represents the fitted curve and the dotted lines represent individual fitting curves. The Raman spectra of the $H_g(1)$ mode of the C_{60} crystal where the fundamental mode of a free molecule is split into three modes at 262, 266, and 272 cm^{-1} is shown for comparison.

($E_{exc}=2.41$ eV) was used. Various interference filters and a prism monochromator served to clean the excitation spectra from plasma lines. The scattered light was analyzed with a SPEX 1877 triple monochromator equipped with a nitrogen cooled CCD detector in 180° back scattering geometry. To avoid any photodegradation effect observed on powder samples,[13] the laser light was focused on the sample with a cylindrical lens and its power density was limited to 10 W/cm^2. We used 1800/mm grating for analysis of the peak structure and 600/mm grating for polarization measurements.

To prevent structural defects, crystals were not cleaved and the Raman spectra were taken from natural crystal faces (mainly {111}) in the case of C_{60} single crystals whereas the TDAE-C_{60} crystals were not oriented.

Since the signal-to-noise ratio of the Raman spectra in *VH* polarization was rather low, the integral intensities of some weak modes were calculated with the fixed peak position and width obtained earlier for *HH* polarization. The Raman data were fitted with the sum of Lorentzian lines and a linear background using commercial PC programs. The positions and full widths at half maximum (FWHM) of the reported Raman lines were obtained as results of the fitting procedure.

III. RESULTS AND DISCUSSION

The Raman spectrum of the TDAE-C_{60} crystal at 10 K shown in Fig. 1 covers the whole frequency range of the fundamental internal modes of the C_{60} molecule. If we compare it with the well-known spectrum for a C_{60} single crystal at the same temperature (also shown in Fig. 1) one can see

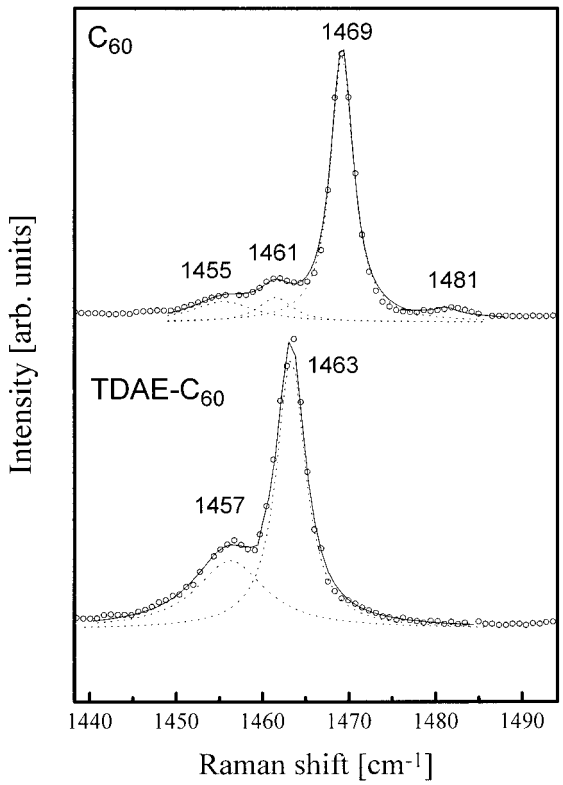

FIG. 3. Raman spectra of the penthagonal pinch mode of the TDAE-C_{60} single crystal compared to C_{60} measured at 10 K. The experimental data are represented by circles, while the dotted lines show the individual fitted curves and the solid lines are the resultant fitted curves.

that the main features in both spectra are very similar. There are two dominating A_g modes and eight much less intense, broadened and split bands in the vicinity of the H_g modes of pristine C_{60}. Since the Raman spectrum of the TDAE-C_{60} crystal deviates from the spectrum of the C_{60} molecule only

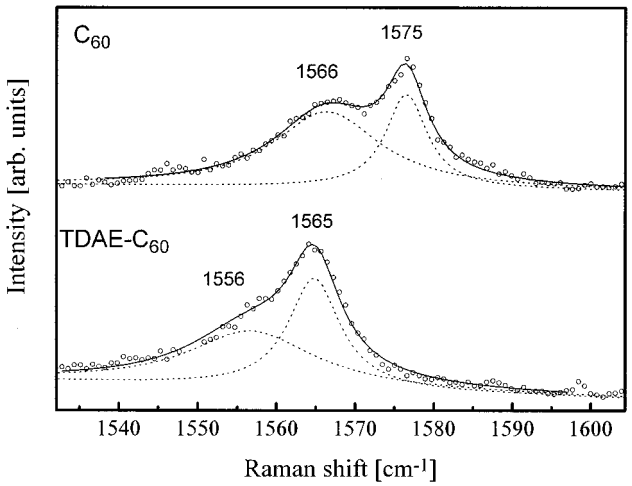

FIG. 4. Raman spectra of the $H_g(8)$ mode of the TDAE-C_{60} single crystal compared to C_{60} measured at 10 K. The experimental data are represented by circles, while the dotted lines show the individual fitted curves and the solid lines are the resultant fitted curves.

TABLE II. Red shift of the Raman lines of TDAE-C_{60} crystal at 10 K compared to (a) the shift in lines observed in the fcc high temperature phase of RbC_{60} crystals at 450 K reported by Winter and Kuzmany (Ref. 9) and (b) to normalize shift in M_xC_{60} presented by Eklund *et al.* (Ref. 15). The shift of the Raman lines in the case of (a) and (b) is relative to the position of Raman lines of C_{60} at temperatures 450 and 300 K, respectively.

I_h mode	C_{60} $T=10$ K ω (cm^{-1})	TDAE-C_{60} $T=10$ K $\Delta\omega$ (cm^{-1})	RbC_{60}[(a)] $T=450$ K $\Delta\omega$ (cm^{-1})	K_3C_{60}[(b)] $T=300$ K $\Delta\omega$ (cm^{-1})	K_6C_{60}[(b)] $T=300$ K $\Delta\omega$ (cm^{-1})	Rb_6C_{60}[(b)] $T=300$ K $\Delta\omega$ (cm^{-1})	Cs_6C_{60}[(b)] $T=300$ K $\Delta\omega$ (cm^{-1})
$A_g(1)$	496	±1	+2	+1	+1.5	+1	+0.5
$A_g(2)$	1469	-6 ± 1	−7	−5	−6	−6	−6
$H_g(1)$	272	-2 ± 1	1	0	0	0	0
$H_g(2)$	433	±1	−9	0	−1.5	−1.5	−1.5
$H_g(4)$	773	−4	−4	-	−2	−2	−2
$H_g(5)$	1100	±1	−4	-	−1	−1.5	−1.5
$H_g(7)$	1424	−4	−15	−6	−7	−7	−7
$H_g(8)$	1566	−10	-	-	-	-	-
	1575	−10	−18	−9	−16	−15	−14

slightly, we can assume that the crystal field influence on the internal symmetry of the C_{60} ion is weak and describe TDAE-C_{60} modes as derived from the corresponding C_{60} modes.

The frequencies of the observed Raman modes, their FWHM and relative intensities together with our data for a C_{60} single crystal (at 10 K) and the Raman data of Denisov *et al.* obtained on a powder sample of TDAE-C_{60} (using 1064 nm laser excitation at 300 K) (Ref. 12) are presented in Table I. Relative intensities have been normalized with respect to the intensity of the radial $A_g(1)$ mode at 496 cm^{-1} since the intensity of the strongest tangential pinch mode $A_g(2)$ at 1463 cm^{-1} varies considerably from one spot on the crystal to another while the former does not.

The polarization study has shown that the ratio $I_{VH}/I_{HH}=0.1$ of the $A_g(2)$ mode of TDAE-C_{60} is close to this value in the pristine C_{60}.[15] Interestingly the strong selection rule for the radial $A_g(1)$ in C_{60} ($I_{VH}/I_{HH}=0.02$) is considerably weakened in TDAE-C_{60} and becomes similar in magnitude to that of the $A_g(2)$ mode. The same violation of the polarization selection rule for the radial $A_g(2)$ mode was observed in M_6C_{60} and was interpreted as the result of the sensitivity of the C_{60} ion symmetry to ball-alkali-metal distance during the radial vibration.[15] Apparently in TDAE-C_{60} the violation of the selection rule for the $A_g(1)$ mode is a manifestation of symmetry breaking arising from an anharmonic potential caused by short contacts between C_{60} and TDAE.

In contrast, the depolarization ratios for H_g-derived modes are comparable with their values in the pristine C_{60}.[15] Taking into account the recent assignment of the optically silent modes for the C_{60} crystal,[16] two weak features at 484 and 760 cm^{-1} can be assigned to the $G_g(1)$ and $H_g(1)\oplus G_g(1)$ even parity vibration and combination mode, respectively (see the last rows of Table I). The weak band at 1084 cm^{-1} is probably the odd parity mode $G_u(4)$ also observed in the C_{60} Raman spectrum.

Comparing the peak positions of TDAE-C_{60} and C_{60} Raman modes one can see that modes with mainly radial character of carbon displacements [$A_g(1)$, $H_g(1,2,3)$] are downshifted in frequency much less (or not shifted at all) than the high frequency modes $A_g(2)$ and $H_g(7,8)$ with predominantly tangential character.[17] The Raman spectrum of TDAE-C_{60} and C_{60} (for comparison) in the regions of the radial (70%) $H_g(1)$ mode and tangential (100%) $A_g(2)$ and (99%) $H_g(8)$ mode are shown in Figs. 2–4, respectively. The analogous behavior of the Raman modes observed earlier in the spectra of alkali-metal-doped C_{60} compounds was explained by a charge transfer related effect,[18] whereby the electron transfer into aromatic rings stretches out the C-C bonds and decreases the tangential mode frequencies, while the frequencies of the radial modes mainly depend on the angle bending force constants which remain unchanged upon doping.

In Table II the shift values of A_g and high frequency H_g modes of TDAE-C_{60} are compared with these values for the corresponding modes in M_nC_{60} compounds.[15] For $n>1$ the shift value is normalized per one electron transferred from the alkali metal. The quite good agreement between the shift values is observed for A_g and $H_g(1)$, $H_g(4)$ modes. The higher values of the shifts that were reported for $H_g(2)$, $H_g(5)$, $H_g(7)$, and $H_g(8)$ modes in RbC_{60} (Ref. 15) can be explained by some uncertainty in the determination of these modes' positions due to their low intensity and broadening. Some discrepancy with M_6C_{60} data might be the consequence of nonlinear behavior of the shift with $n>3$ since our data correspond quite well with K_3C_{60}.

Comparing the effects of resonance on our results with the data of Denisov *et al.*,[12] who performed Raman spectroscopy at $\lambda=1.06$ μm (last column in Table I), we can see that positions of the tangential modes ($w>700$ cm^{-1}) correspond well in the two cases, but there are big differences in the frequencies of the radial modes. According to Denisov *et al.*[12] all radial modes are downshifted near 7 cm^{-1}, which is not observed with 514.5 nm excitation.

We suggest that the origin of this effect is related to the involvement of different Frank-Condon shifted levels in resonances at 1.06 μm and 514.5 nm, respectively, in photoexcited C_{60}^-.[19,20] Upon resonant photoexcitation, a relaxed state, denoted as C_{60}^{-*}, is created by the incident photon

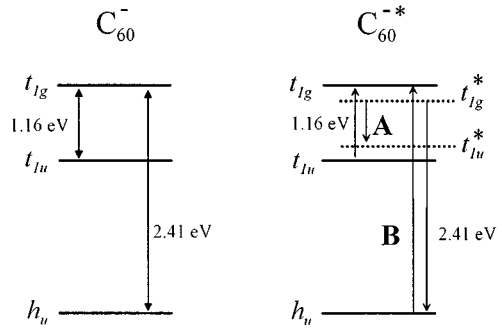

FIG. 5. Schematic representation of the Raman resonance for 1.16 and 2.41 eV excitation with the $t_{1u}^* \rightarrow t_{1g}^*$ and $h_u \rightarrow t_{1g}^*$ levels, respectively.

creating new t_{1u}^* HOMO and t_{1g}^* LUMO levels derived from the original t_{1u} and t_{1g} levels of the unexcited anion. The suggested Raman transitions between such states are shown in Fig. 5 (only electronic levels are indicated for simplicity). In the Herzberg-Teller formulation, for $E_{\text{exc}}=1.16$ eV, the first exciting transition would be $t_{1u} \rightarrow t_{1g}$, and the second from t_{1g}^* to the t_{1u}^* vibronically modified ground state. Since the relaxation of the t_{1g}^* and t_{1u}^* levels results also in modified vibration frequencies, we observe a shift in the radial and tangential mode frequencies. A slightly different set of transitions is involved for $E_{\text{exc}}=2.41$ eV (transition *B* in Fig. 5), where the unrelaxed HOMO-1 h_u is the inital state, the t_{1g} and t_{1g}^* are intermediate states, and h_u the final state. In this case only tangential modes are shifted. Combining the fact that tangential modes shift for both excitation wavelengths, and the common intermediate state in both resonance experiments is the t_{1g}^* level, we can infer that the shift of the tangential modes arises because of vibronic coupling to the relaxed t_{1g}^* level. The corollary is that the shift of the radial modes arises due to coupling to the t_{1u}^* ground state.

The spectrum in the vicinity of the $A_g(2)$ mode was previously found to be very sensitive to laser power[13] and also to be very sample dependent.[21] As a result it was difficult to make a reliable assignment of the pinch-mode spectra on the basis of powder spectra even with the lowest laser powers.[13] To clarify the influence of TDAE-C_{60} exposure to air, we have measured the Raman spectra of three crystals, progressively more exposed to air. Sample *A* was stored in air for 4 days before measurement, sample *B* was cleaved in air and immediately put into the cryostat, while sample *C* was both cleaved and mounted in a glove bag with a 15 min purge of He gas to reduce the O_2. The spectra of these crystals are compared with the spectra of samples which were handled with extreme care in a glovebox with $O_2<1$ ppm in Fig. 6. Dramatic changes are observed in the shape of the spectrum upon the air exposition. The sharp narrow $A_g(2)$ line at 1463 cm^{-1} of uncontaminated TDAE-C_{60} becomes three times broader in the spectrum of sample *C* showing that even the slightest exposure to air completely changes the spectrum in this region. With further exposition (sample *B*) the intensity of the $A_g(2)$ line drops and a sharp line at the position of $A_g(2)$ mode in the pristine C_{60} (1469 cm^{-1}) appears while in the spectrum of the strongly contaminated sample *A*, only two broad features (FWHM ~ 50 cm^{-1}) with broad maxima at 1435 and 1462 cm^{-1} are observed. We note that only the sharp line at 1463 cm^{-1} is intrinsic, while the broad feature

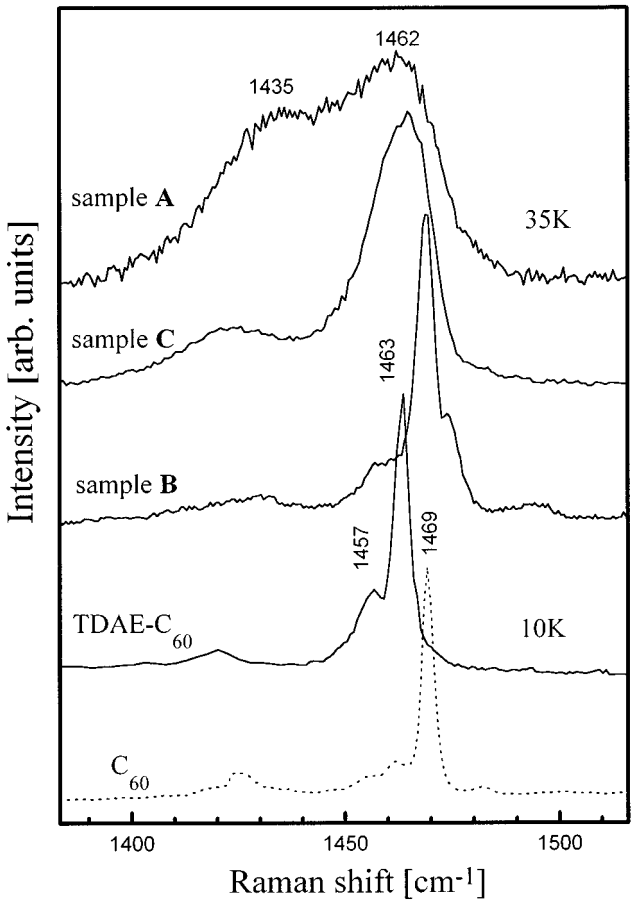

FIG. 6. Raman spectra in the region of the $A_g(2)$ mode of TDAE-C_{60} for four different crystals: (TDAE-C_{60}) represents the spectrum of the crystal that was not exposed to air, samples *A*, *B*, *C* were exposed to air for different times (see text); the spectrum of C_{60} is presented for comparison.

at the same frequency in contaminated samples is not (sample *C*), and is most probably a superposition of $TDAE^+C_{60}^-$ and C_{60} lines.

IV. CONCLUSIONS

The Raman spectra of TDAE-C_{60} single crystals were studied with 514.5 nm (2.41 eV) excitation at temperatures well below the temperature of orientation ordering transition, avoiding possible photopolymerization effects. Very few additional optical modes over those anticipated from I_h symmetry of the C_{60}^- ion were observed which can be considered as an evidence for weak intermolecular coupling in TDAE-C_{60}. High frequency *tangential* modes of TDAE-C_{60} exhibit a softening similar as in alkali-doped fullerene compounds which is attributed to elongation of C-C bonds in aromatic rings,[18] which is in contrast to the behavior observed by Denisov *et al.*[12] with 1.06 μm resonant excitation, where both tangential and radial modes shift in frequency. The effect is attributed to selective Raman resonance with two different sets of Frank-Condon relaxated states of the C_{60}^- molecule, one resonant with the $t_{1u} \rightarrow t_{1g}$ transition near 1 eV and the other with the $h_u \rightarrow t_{1g}$ transition at 2.4 eV.

*On leave from Institute of Semiconductors, Kiev, Ukraine.
[1] P.M. Allemand, K.C. Khemani, A. Koch, F. Wudl, K. Holczer, S. Donovan, G. Gruner, and J.D. Thompson, Science **301**, 253 (1991).
[2] L. Golic, *Proccedings of the International Winter School on Fullerenes and Fullerene Nanostructures* (Kirchberg, Austria, 1996).
[3] S. Pekker, L. Forro, L. Mihaly, and A. Janossy, Solid State Commun. **90**, 349 (1994).
[4] K. Tanaka *et al.* Phys. Rev. B **47**, 7554 (1993).
[5] A. Omerzu, D. Mihailovic, S. Tomic, and N. Biskup, Phys. Rev Lett. **77**, 2045 (1996).
[6] R. Blinc *et al.* Phys. Rev. Lett. **76**, 523 (1996).
[7] D. Arcon, J. Dolinsek, R. Blinc, K. Pokhodnia, A. Omerzu, D. Mihailovic, and P. Venturini, Phys. Rev. B **53**, 14 028 (1996).
[8] D. Mihailovic, D. Arcon, P. Venturini, R. Blinc, A. Omerzu, and P. Cevc, Science **268**, 400 (1995).
[9] J. Winter and H. Kuzmany, Phys. Rev. B **52**, 7115 (1995).
[10] Y. Iwasa, T. Arima, R.M. Fleming, T. Siegrist, O. Zhou, R.C. Haddon, L.J. Rothberg, K.B. Lyons, H.L. Carter, Jr., A.F. Hebard, R. Tycko, G. Dabbagh, J.J. Krajewski, G.A. Thomas, and T. Yagi, Science **264**, 1570 (1994).
[11] D.S.V. Muthu, M.N. Shashikava, A.K. Saad Ram Seshadri, and C.N.R. Rao, Chem. Phys. Lett. **217**, 146 (1994).
[12] V.N. Denisov, A.A. Zakhidov, G. Ruani, R. Zamboni, C. Taliani, K. Tanaka, K. Yoshizawa, T. Okahara, T. Yamabe, and Y. Achiba, Synth. Met. **55-57**, 3050 (1993).
[13] D. Mihailovic, P. Venturini, A. Hassanien, J. Gasperic, K. Luthar, S. Milicev, and V. Srdanov, in *Electronic Properties of Novel Materials: Progress in Fullerene Research*, edited by H. Kuzmany, J. Fink, M. Mehring, and S. Roth (World Scientific Publishing, Singapore, 1994), p. 275.
[14] H. Kuzmany, M. Matus, B. Burger, and J. Winter, Adv. Matter **6**, 731 (1994).
[15] P.C. Eklund, P. Zhou, Kai-Au Wang, G. Dresselhaus, and M.S. Dresselhaus, J. Phys. Chem. Solids **53**, 1391 (1992).
[16] K.A. Wang, A.M. Rao, P.C. Eklund, M.S. Dresselhaus, and G. Dresselhaus, Phys. Rev. B **48**, 11 375 (1993).
[17] R.E. Stanton and M.D. Newton, J. Phys. Chem. **92**, 2141 (1988).
[18] R.A. Jishi and M.S. Dresselhaus, Phys. Rev. B **45**, 2597 (1992).
[19] T. Kato, T. Kodama, M. Oyama, S. Okazaki, T. Shida, T. Nakagawa, Y. Matsui, S. Suzuki, H. Shivomaru, K. Yamauchi, and Y. Achiba, Chem. Phys. Lett. **186**, 35 (1991).
[20] A.S. Alexandrov and V.V. Kabanov, Pis'ma Zh. Éksp. Teor. Fiz. **62**, 920 (1995) [JETP Lett. **62**, 937 (1995)].
[21] D. Mihailovic, K. Lutar, A. Hassaninen, P. Cevc, and P. Venturini, Solid State Commun. **89**, 209 (1994).